



Published in final edited form as:

ACS Chem Biol. 2010 February 19; 5(2): 233–243. doi:10.1021/cb900232a.

## Development of near-infrared fluorophore (NIRF)-labeled activity-based probes for *in vivo* imaging of legumain

Jiyoun Lee and Matthew Bogyo

Departments of Pathology and Microbiology and Immunology, Stanford University School of Medicine, 300 Pasteur Dr. Stanford, CA 94305-5324

### Abstract

Asparaginyl endopeptidase, or legumain, is a lysosomal cysteine protease that was originally identified in plants and later found to be involved in antigen presentation in higher eukaryotes. Legumain is also up-regulated in a number of human cancers and recent studies suggest that it may play important functional roles in the process of tumorigenesis. However, detailed functional studies in relevant animal models of human disease have been hindered by the lack of suitably selective small molecule inhibitors and imaging reagents. Here we present the design, optimization and *in vivo* application of fluorescently labeled activity based probes (ABPs) for legumain. We demonstrate that optimized aza-peptidyl Asn epoxides are highly selective and potent inhibitors that can be readily converted into NIRF labeled ABPs for whole body, non-invasive imaging applications. We show that these probes specifically label legumain in various normal tissues as well as in solid tumors when applied *in vivo*. Interestingly, addition of cell penetrating peptides to the probes enhanced cellular uptake but resulted in increased cross-reactivity towards other lysosomal proteases as the result of their accumulation in lysosomes. Overall, we find that aza-peptidyl Asn ABPs are valuable new tools for the future study of legumain function in more complex models of human disease.

### Keywords

Activity based probes; legumain; fluorescence imaging; NIRF probes; protease inhibitors

---

Asparaginyl endopeptidase, also known as legumain, is a lysosomal cysteine protease that was named based on its propensity to cleave protein substrates on the C-terminal side of asparagine residues (1). Legumain is expressed in diverse cell types, and in most cases, its functions are unknown. Recently legumain has emerged as an important enzyme in antigen processing (2, 3) and matrix degradation (4, 5) and it is implicated in various pathological conditions including parasite infection (6, 7), atherosclerosis (8) and tumorigenesis (9, 10). For example, legumain is heavily over-expressed in the majority of human solid tumors such as carcinomas of the breast, colon and prostate (9). Furthermore, knock-down of legumain in mouse models of cancer resulted in a marked decrease in tumor growth and metastasis (10). More recently, mice lacking legumain develop disorders similar to hemophagocytic syndrome, a form of hyperinflammatory response (11). Despite the mounting evidence of legumain as a therapeutically important target, especially in tumor progression and metastasis, current methods to study legumain function mainly depend on antibodies and genetic modification, making it difficult to study legumain in its native state.

---

Correspondence: Matthew Bogyo mbogyo@stanford.edu Phone: 650-725-4132 FAX: 650 – 725-7424.

**Supporting Information Available:** This material is available free of charge via the Internet at <http://pubs.acs.org>.

Small molecule chemical tools such as activity-based probes (ABPs) provide a highly versatile means to monitor protease function and regulation in a wide range of biological systems. Typical ABPs utilize irreversible inhibitors that can covalently modify active site of enzyme in an activity dependent fashion. However, only a few legumain-specific inhibitors have appeared in the literature thus far. All of these inhibitors have a Cbz-Ala-Ala-Asn peptide scaffold that is based on the sequence of a known substrate of legumain (12). In addition, a number of different reactive electrophilic functional groups including aza-Asn halomethylketones (13), aza-Asn epoxides (7) and aza-Asn Michael acceptors (6) have been used to make irreversible legumain inhibitors. Although these inhibitors are highly potent against legumain *in vitro*, their potency, and more importantly, their selectivity *in vivo*, has never been tested. We have previously developed a cell-permeable ABP for legumain that is composed of a peptide acyloxymethyl ketone (AOMK) with a P1 aspartic acid (14). Although this probe is useful to study active legumain in cells, it has overall poor potency and can readily cross react with caspases, which also optimally bind to aspartic acid containing AOMKs (15). We therefore decided to develop a new class of legumain inhibitors with faster kinetic properties and increased selectivity for legumain for use in *in vivo* imaging studies. Herein, we present a new class of aza-Asn epoxide ABPs for legumain that are labeled with Cy5 fluorophore and also tagged with a series of cell-permeabilizing groups. This new generation of legumain probes can be used to image active legumain both in normal tissues and within solid tumors.

## RESULTS AND DISCUSSION

### Design of legumain probes for *in vivo* applications

In order to develop new tools to study legumain function *in vivo* we needed to identify a scaffold that could be used to make probes that were highly selective for legumain with virtually no cross reactivity for other lysosomal proteases or related CD clan proteases such as caspases. In the past, our group developed activity based probes that can be used to label legumain in cell culture models (14). These first generation probes make use of the acyloxymethyl ketone (AOMK) group to covalently modify the active site cysteine and a Pro-Asp peptide for specific recognition by legumain. This peptide sequence was chosen based on the finding that, although legumain prefers processing of substrates at asparagine residues, it also binds to probes with a P1 aspartic acid (16). Since P1 Asn AOMKs are highly unstable (17), we originally focused our attention on the P1 Asp AOMK probes. These reagents, while useful for labeling legumain, have overall slow binding properties and generally low potency. In addition, P1 Asp-AOMKs are highly effective labels of caspases both *in vitro* and *in vivo* (18, 19). Recent reports suggest that aza-peptidyl epoxides can be designed to be highly potent inhibitors of legumain with overall low cross-reactivity toward other lysosomal cystein proteases such as the cathepsins (7). The unique aza scaffold also allows incorporation of a P1 Asn residue without causing overall instability of the compound. Based on these findings, we envisioned that aza-Asn epoxide should be valuable for use in imaging probes due to very low reactivity towards cathepsins and caspases. We therefore synthesized an activity based probe LP-1 (Legumain Probe -1) that contains the aza-Asn epoxide and the P2 Pro of the first generation AOMK probe as well as a Cy5 fluorophore for *in vivo* imaging applications (Figure 1a). We also synthesized a Cy5-labeled version of the previously reported probe Biotin-PD-AOMK (LP-0, Figure 1a) for direct comparison with LP-1. LP-1 was synthesized via a previously reported solid-phase synthesis technique (20) and the Cy5 fluorophore was conjugated to the purified peptide at the final step (Scheme 1). To directly compare enzyme specificity and kinetics between LP-1 and the previously described AOMKs, we also synthesized acetyl-capped inhibitor versions of LP-1 and LP-0 (LI-1 and LI-0 respectively; Figure 1a).

## Selectivity and potency of legumain inhibitors and probes

To determine the overall potency and selectivity of the aza-epoxide and AOMK inhibitors we performed inhibition studies for both compounds against recombinant legumain, cathepsin B, cathepsin L and caspase-3 (Table 1). Simple  $IC_{50}$  determination showed that LI-1 ( $IC_{50} = 11.5$  nM) is 70-fold more potent than LI-0 ( $IC_{50} = 704$  nM) against legumain, while both compounds showed very weak activity against cathepsin B ( $IC_{50} = 390$   $\mu$ M for LI-1 and greater than 1mM for LI-0) and cathepsin L ( $IC_{50} = 202$   $\mu$ M for LI-1 and higher than 1mM for LI-0). Importantly, LI-0 showed a significant inhibitory effect ( $IC_{50} = 2.8$   $\mu$ M) on caspase-3 while LI-1 showed nearly no inhibition ( $IC_{50} = 890$   $\mu$ M). To further evaluate the kinetics of inhibition of legumain by the two classes of inhibitors we also measured second-order rate constants ( $k_{obs}/[I]$ ) for both compounds (Table 1). As expected, LI-1 ( $k_{obs}/[I] = 72350$   $M^{-1}s^{-1}$ ) inhibited legumain approximately 50-fold faster than LI-0 ( $k_{obs}/[I] = 1585$   $M^{-1}s^{-1}$ ). These results confirmed that incorporation of P1 Asn via aza-peptidyl scaffold greatly enhanced efficiency and specificity of inhibition by LI-1 compared to the P1 Asp AOMK scaffold. The rapid inhibition kinetics of the aza-Asn epoxide scaffold is advantageous for *in vivo* imaging as it allows rapid binding to legumain thus providing a better signal to noise ratio even for probes with relatively short half-lives *in vivo*. This allows the use of lower overall doses of probe and prevents extended circulation that can possibly cause cross reactivity with other proteases.

We next wanted to verify labeling of active legumain in intact cells. Therefore, we treated intact NIH-3T3 and RAW 264.7 cells with LP-1 and LP-0 respectively and monitored protein labeling using SDS-PAGE followed by scanning of the gel to detect the Cy5 fluorescence (Figure 1b). Both probes selectively labeled active legumain in NIH-3T3 fibroblasts. As previously observed in the enzyme kinetic assays, LP-1 labeled active legumain more efficiently than LP-0 at low probe concentrations and showed overall stronger labeling signals. Interestingly, when the two probes were used to label RAW 264.7 macrophages, both showed some degree of cross reactivity towards lysosomal cathepsins. The identity of these off targets as cathepsins was confirmed by pre-treatment of cells with the broad-spectrum cathepsin inhibitor JPM-OEt (21) and further verified by immunoprecipitation (Supplementary Figure S1). Although some degree of cross reactivity of AOMK probes towards cathepsins has been reported (15), attempts to inhibit cathepsins with various aza-epoxide inhibitors have been unsuccessful (22). Therefore, the labeling of cathepsins by LP-1 was particularly surprising. These data suggest that even though compounds may have very low potency toward a particular protease target *in vitro*, when added to cells that actively accumulate the probes in their lysosomes, such as macrophages, they are able to react with other abundant proteases. Furthermore, when cells were pre-treated with legumain inhibitors we observed more intense cathepsin labeling. This could be explained by the fact that cathepsins are known to be substrates for legumain (3, 23), thus legumain inhibition could result in increased levels of cathepsins and therefore increased non-specific labeling by the legumain probes. While the cathepsin cross reactivity is not ideal, by using lower probe concentrations and more potent inhibitor scaffolds, it should be possible to obtain selective labeling of legumain *in vivo*. Based on these results, we decided that LP-1 would be the optimal reagent for *in vivo* imaging studies as it has faster kinetics and its overall higher potency, resulting in less background labeling of cathepsins and caspases.

### *In vivo* imaging of legumain using the aza-epoxide probe LP-1

In order to examine *in vivo* properties of LP-1 and monitor active legumain levels non-invasively, we performed imaging experiments using a simple tumor xenograft model (C2C12/Hras1)(24). To verify that the *in vivo* fluorescent signal from LP-1 is legumain-specific we also used a control probe (LP-1 ctrl, see supporting information) that lacks the

reactive epoxide group and therefore does not covalently bind to legumain. Mice were injected with the probes via tail vein and fluorescent images were collected over the course of 5 hrs. As expected, LP-1 rapidly accumulated in tumor tissues whereas LP-1 ctrl did not show such accumulation (Figure 2a). Quantification of the tumor to normal tissue ratio from the fluorescent images showed that LP-1 accumulated in tumors with a maximum signal to background ratio obtained at around 90 min (Figure 2b). Furthermore, the specific legumain signal declined over time but remained significantly higher than the signal observed for the control probe even at the longer time points. This labeling pattern is in contrast to the previously reported cathepsin probes which only provide contrast after 8–12 hours and signals are retained beyond 48 hours. These data suggesting that legumain may have a more rapid rate of turn-over than the cathepsins and that the legumain probes have faster binding and clearance properties that leads to more rapid signal over background.

At the end of the imaging time-course, we collected organs and carried out *ex vivo* imaging and SDS-PAGE analysis of extracts to confirm selective labeling of legumain by LP-1 (Figure 2c). Importantly, fluorescent images of each tissue showed that levels of active legumain directly correlated with the intensity of legumain labeling as measured by SDS-PAGE analysis. The result also demonstrated that LP-1 is remarkably selective toward legumain *in vivo* and showed virtually no off-target labeling. These data further support our hypothesis that using a more potent and kinetically fast binding scaffold, allows selective labeling of legumain *in vivo*.

### Use of a tat peptide to increase cellular uptake

Previously we reported that conjugating the tat peptide to an activity-based probe that targets caspases enhanced cell-permeability, however, it also increased lysosomal uptake due to its positive charge. Thus the use of the tat carrier inadvertently increased cross-reactivity toward legumain (18). Inspired by this result, we conjugated the tat peptide to LP-1 to further improve its *in vitro* and *in vivo* reactivity toward legumain. To our surprise, when tested against intact RAW 264.7 macrophages, tat conjugated LP-1 (tLP-1; Figure 3a) labeled not only legumain but also multiple cathepsins, even at low concentrations (Figure 3b). We believe that this cross-reactivity results from increased lysosomal uptake and is not the result of a loss of specificity as the result of addition of the tat peptide. To test this hypothesis, we labeled RAW cell lysates with LP-1 and tLP-1 (Figure 3c). SDS-PAGE analysis confirmed that there is no difference in reactivity towards legumain for these two probes. We also performed a competition assay by pretreating RAW lysates with each probe and labeling with the general cathepsin probe, I<sup>125</sup>-DCG04 (25). These results further confirmed that both LP-1 and tLP-1 are equally poor inhibitors of the cathepsins (Figure 3d). Thus, the increased cross reactivity towards cathepsins is likely due to significant accumulation of the tLP-1 in the lysosome.

Since tLP-1 showed high cross-reactivity toward cathepsins in cells, we wanted to monitor its *in vivo* distribution and labeling kinetics compared to LP-1. We performed *in vivo* imaging and found that, although the tat peptide enhanced overall uptake of the probe, tLP-1 failed to show the selective uptake in tumors observed for LP-1. In addition, the tat peptide dramatically increased overall probe distribution and reduced the rate of clearance (Figure 4a). As a result, tLP-1 showed increased non-selective labeling *in vivo* relative to LP-1 (Figure 4b).

### Use of additional carrier-conjugates on legumain probes

Cell-penetrating peptides (CPPs) and membrane targeting moieties have proven to be useful delivery methods for various biological reagents (26, 27). In addition to the tat peptide, we also decided to test several additional carrier molecules with our legumain probes. We chose

octa-arginine (r8) and penetratin due to their widespread use as carriers. We also chose cholesterol since it has high affinity for membrane raft domains and has been used to enhance membrane permeability (28) (Figure 5a).

To compare differences in cell permeability and labeling efficiency between these probes, we treated intact cells with each conjugate and analyzed labeling by SDS-PAGE. As previously observed for tLP-1, all the carrier-conjugates showed increased cellular uptake resulting in stronger labeling but also more cross-reactivity (Figure 5b). All CPP conjugated probes, tLP-1, r8 LP-1 and penetratin LP-1 showed almost identical protein labeling profiles indicating that all of these probes are delivered by similar mechanisms and are enriched in lysosomes. Cholesterol LP-1 showed enhanced legumain labeling with less cross-reactivity suggesting that membrane anchoring cholesterol helped selective delivery of LP-1. Next, we carried out *in vivo* imaging experiments with penetratin-LP-1 and cholesterol-LP-1 to compare their *in vivo* distribution to LP-1 (Figure 6a). Although the carrier labeled probes accumulated in tumors to some extent, their slow clearance resulted in low tumor to background levels (Figure 6b). *ex vivo* imaging of the collected organs followed by analysis of lysates by SDS-PAGE as confirmed that carrier labeled probes suffered from increased cross reactivity with cathepsin proteases (Figure 6c). Overall, LP-1 showed the most legumain labeling in tumors as well as the highest levels of legumain-specific fluorescent signal whereas penetratin LP-1 and cholesterol LP-1 showed non-specific distribution in most organs and much higher cross reactivity toward cathepsins. We believe that enhanced cellular delivery of these probes adversely affects overall circulation of the probe resulting in less useful imaging reagents. Furthermore, all of the carrier molecules caused increased association with tissues other than the target tumors suggesting that legumain ABPs are more effective as free probes that do not contain a carrier peptide.

In conclusion, we have developed a NIRF-labeled legumain probe, LP-1, based on a highly potent and selective inhibitor. The probe contains a Pro-Asn-aza epoxide scaffold that is distinct from the previously reported legumain inhibitors. When LP-1 was used for non-invasive imaging applications, we were able to monitor legumain activity both in normal tissues and in solid tumors. Its favorable reactivity and clearance resulted in high contrast in tumors rapidly after probe injection. We were also able to track whole body distribution of the probe as well as the level of active legumain in organs by *ex-vivo* imaging and SDS-PAGE. In addition, we tested a series of cell-permeabilizing moieties as a delivery strategy for ABPs. Although some of these moieties improved cell permeability and legumain labeling in cells, they also increased off-target labeling via enhanced lysosomal uptake and extended circulation times *in vivo*. We conclude that LP-1 is a valuable new imaging probe with desirable *in vitro* and *in vivo* characteristics. While this probe can be used for non-invasive imaging studies it also has great potential value for invasive applications in which direct assessment of levels of active legumain in whole tissues or cells *in vivo* are required. This new imaging agent and its corresponding inhibitor are likely to prove valuable for future *in vivo* studies of legumain function.

## METHODS

### General methods

Unless otherwise noted, all resins and reagents were obtained from commercial suppliers and used without further purification. All solvents used were HPLC-grade and also purchased from commercial suppliers. Reactions were analyzed by LC/MS performed on an Agilent 1100 liquid chromatography system with an API 150EX single quadrupole mass spectrometer (Applied Biosystems). HPLC purifications were carried out using an ÄKTA explorer 100 (Amersham Pharmacia Biotech) with C<sub>18</sub> reversed-phase columns (Waters). Mobile phase consisted of 95:5:0.1 = water: acetonitrile: trifluoroacetic acid (solvent A) and

0.1% trifluoroacetic acid in acetonitrile (solvent B). High-resolution mass spectrometry (HRMS) was performed using an LTQ-FTMS (Thermo Fisher Scientific). Matrix-assisted laser desorption ionization time of flight (MALDI-TOF) mass spectrometry was performed using a Bruker Autoflex TOF/TOF mass spectrometer (Bruker). IC<sub>50</sub> measurements and enzyme kinetics assays were performed on a Spectramax M5 fluorescent plate reader (Molecular Devices). Fluorescent gels were scanned with a Typhoon 9400 flatbed laser scanner (GE Healthcare). Male BALB/c nude mice (4–8 weeks old) were obtained from Charles River and housed in the research animal facility at the Stanford University Department of Comparative Medicine. All animal protocols were approved by the Stanford Administrative Panel on Laboratory Animal Care, and the procedures were performed in accordance to their guidelines. *In vivo* imaging experiments were performed using the IVIS 200 imaging system (Xenogen) and *ex vivo* imaging experiments were performed using the FMT 2500 system (VisEn Medical).

### Synthesis and characterization

Peptidyl Aza-Asn epoxide was synthesized by following the previously reported procedure (20) on a Rink SS resin (Advanced ChemTech). Peptidyl Asp AOMK was synthesized by the previously reported procedure (15). Each carrier-probe conjugate was synthesized by following the previously reported procedure (18). The tat peptide and the penetratin peptide were custom synthesized by the Stanford PAN peptide synthesis facility. All synthesized peptides were cleaved from resin by applying cleavage cocktail containing 95% TFA and purified by HPLC. The purified peptides were then coupled with Cy5-NHS (1eq) in DMSO with DIEA (5eq) for 1hr and purified by HPLC. The purity and identity of all compounds were assessed by LC-MS and HR-MS. Detailed synthetic procedures and characterization data of final compounds can be found in the supporting information.

### Determination of IC<sub>50</sub> against cysteine proteases and second order rate constants ( $k_{obs}/[I]$ ) for legumain

Activity of legumain was measured with the fluorogenic substrate, Cbz-Ala-Ala-Asn-AMC (Anaspec), cathepsin B and cathepsin L was measured with Cbz-Phe-Arg-AMC (Bachem), and caspase-3 was measured with Caspase-3 Substrate VII (Calbiochem). Assay buffers consist of 20mM citric acid, 60mM disodium hydrogen orthophosphate, 1mM EDTA, 0.1% CHAPS, 4mM DTT, pH 5.8 for legumain, 50mM dihydrogen sodium orthophosphate, 1mM EDTA, 5mM DTT, pH 6.25 for cathepsin B and cathepsin L and 100 mM Tris, 0.1% CHAPS, 10% sucrose, 10mM DTT, pH 7.4 for caspase-3. Concentrations of substrates during the measurement were 10 $\mu$ M (legumain, cathepsin L and caspase-3) and 50 $\mu$ M (cathepsin B) and concentration of enzymes were 100nM for cathepsin L and caspase-3, 270nM for legumain and 360nM for cathepsin B. Each enzyme was incubated with inhibitor concentrations ranging from 1nM to 1mM in the presence of the substrates. The increase in fluorescence was continuously monitored every 30 sec for 2.5 hrs with a Spectramax M5 fluorescent plate reader (Molecular Devices), and inhibition curves were recorded. IC<sub>50</sub> values were calculated by plotting the normalized enzyme activity against the inhibitor concentration at 60min for legumain and at 30min for caspase-3, cathepsin B and cathepsin L using nonlinear regression analysis (GraphPad Prism). IC<sub>50</sub> values with known broad-spectrum cathepsin inhibitor (JPM-OEt) and caspase-3 inhibitor (Z-DEVD-FMK) were also measured for comparison. All measurements were performed in triplicate and the average values were reported.

Second-order inhibition rate constants were determined by following the previously described method in the literature (6). The pseudo-first-order rate constants ( $k_{obs}$ ) were obtained from plots of  $\ln v_t/v_0$  versus time where  $v_0$  is the rate of hydrolysis of fluorogenic substrate and  $v_t$  is the rate of hydrolysis of substrate in the presence of the inhibitor. The

second-order inhibition rate constants were calculated using the following equation. Second order rate constant =  $(k_{\text{obs}}/[I])(1+[S]/K_m)$

### Direct labeling of endogenous legumain in intact cells and cell lysates

RAW 264.7 cells (250,000 cells/well) and NIH-3T3 cells (200,000 cells/well) were seeded in a 24-well plate 24–30 hrs prior to labeling. Cells were pretreated with appropriate inhibitors for 1.5 hrs and labeled by addition of each probe for 1 hrs; the final DMSO concentration was maintained less than 0.2%. Cells were washed with PBS buffer and lysed by addition of sample buffer. Crude lysates were collected and separated by 12.5% SDS-PAGE. Labeled proteins were analyzed by scanning the gel with a Typhoon flatbed laser scanner (ex.633nm/em.680nm). For lysates labeling, cytosolic lysates of RAW 264.7 cells were prepared as previously described (29). Lysates were diluted to 1mg ml<sup>-1</sup> in 50mM citrate phosphate buffer (pH 4.5), 0.1% CHAPS, 5mM DTT and subjected to direct labeling. 25µL of lysates samples were pretreated with inhibitors for 30 min and labeled with probes for another 30min. The labeled samples were separated by 12.5% SDS-PAGE and analyzed by scanning the gel with a Typhoon flatbed scanner.

### In vivo / ex vivo imaging and SDS-PAGE analysis of organ lysates

Tumor bearing mice were prepared by following the previously described method (24). C2C12/Hras1 or MDA-MB 231 MFP cells ( $2 \times 10^{-6}$  cells/mouse) were injected subcutaneously on 4–8 week old male BALB/c nude mice. 14 days after transplantation, each probe (25 nmol in 100µL of sterile PBS) was injected via the tail vein into tumor-bearing mice. Mice were imaged at various time points after injection using the IVIS 200 imaging system equipped with a Cy5.5 filter. Relative fluorescence of equal-sized areas of tumor and background were measured using Living Image software (Caliper life science). Upon finishing the last time point of imaging, mice were anesthetized and sacrificed by cervical dislocation. Tumors, livers, kidneys and spleens were collected and imaged *ex vivo* by using the FMT 2500 with a Cy5 filter. After *ex vivo* imaging, organs were lysed by a dounce homogenizer in muscle lysis buffer (1% Triton X-100, 0.1% SDS, 0.5% sodium deoxycholate, 0.2% sodium azide in PBS, pH 7.2). Total protein extracts (100µg each) were separated by SDS-PAGE and visualized by scanning the gel with a Typhoon flatbed laser scanner.

## Supplementary Material

Refer to Web version on PubMed Central for supplementary material.

## Acknowledgments

We thank G. Blum and L. Edgington for valuable advice and technical assistance for initial animal experiments. We thank S. Verhelst and V. Albrow for helpful discussions about chemical synthesis. We also thank E. Deu Sandoval for help with enzyme assays, A. Guzzetta for HR-MS analysis, and F. Yin and M. Paulick for helpful discussions about cathepsins and assistance with the immunoprecipitations. This work was supported by an NIH National Technology Center for Networks and Pathways grant U54 RR020843 (to M.B.), NIH grant R01-EB005011 (to MB).

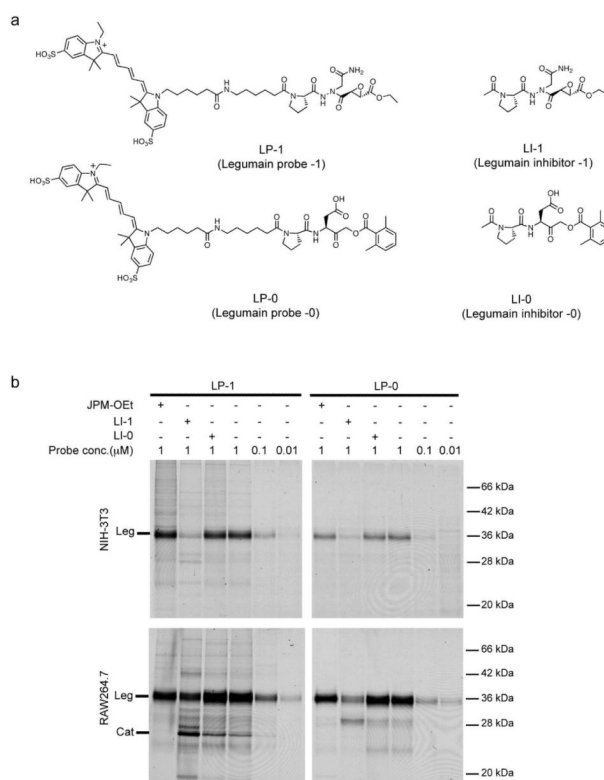
## Reference

1. Ishii S. Legumain: asparaginyl endopeptidase. *Methods Enzymol.* 1994; 244:604–615. [PubMed: 7845236]
2. Manoury B, Mazzeo D, Li DN, Billson J, Loak K, Benaroch P, Watts C. Asparagine endopeptidase can initiate the removal of the MHC class II invariant chain chaperone. *Immunity.* 2003; 18:489–498. [PubMed: 12705852]

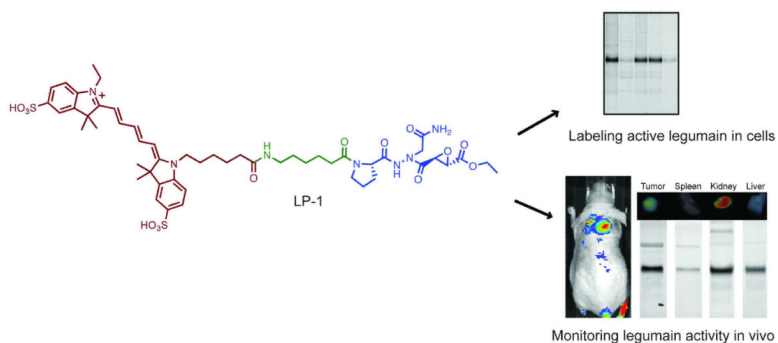
3. Maehr R, Hang HC, Mintern JD, Kim YM, Cuvillier A, Nishimura M, Yamada K, Shirahama-Noda K, Hara-Nishimura I, Ploegh HL. Asparagine endopeptidase is not essential for class II MHC antigen presentation but is required for processing of cathepsin L in mice. *J Immunol.* 2005; 174:7066–7074. [PubMed: 15905550]
4. Morita Y, Araki H, Sugimoto T, Takeuchi K, Yamane T, Maeda T, Yamamoto Y, Nishi K, Asano M, Shirahama-Noda K, Nishimura M, Uzu T, Hara-Nishimura I, Koya D, Kashiwagi A, Ohkubo I. Legumain/asparaginyl endopeptidase controls extracellular matrix remodeling through the degradation of fibronectin in mouse renal proximal tubular cells. *FEBS Lett.* 2007; 581:1417–1424. [PubMed: 17350006]
5. Sottile J, Hocking DC. Fibronectin polymerization regulates the composition and stability of extracellular matrix fibrils and cell-matrix adhesions. *Mol Biol Cell.* 2002; 13:3546–3559. [PubMed: 12388756]
6. Gotz MG, James KE, Hansell E, Dvorak J, Seshadri A, Sojka D, Kopacek P, McKerrow JH, Caffrey CR, Powers JC. Aza-peptidyl Michael acceptors. A new class of potent and selective inhibitors of asparaginyl endopeptidases (legumains) from evolutionarily diverse pathogens. *J Med Chem.* 2008; 51:2816–2832. [PubMed: 18416543]
7. James KE, Gotz MG, Caffrey CR, Hansell E, Carter W, Barrett AJ, McKerrow JH, Powers JC. Aza-peptide epoxides: potent and selective inhibitors of *Schistosoma mansoni* and pig kidney legumains (asparaginyl endopeptidases). *Biol Chem.* 2003; 384:1613–1618. [PubMed: 14719804]
8. Clerin V, Shih HH, Deng N, Hebert G, Resmini C, Shields KM, Feldman JL, Winkler A, Albert L, Maganti V, Wong A, Paulsen JE, Keith JC Jr, Vlasuk GP, Pittman DD. Expression of the cysteine protease legumain in vascular lesions and functional implications in atherogenesis. *Atherosclerosis.* 2008; 201:53–66. [PubMed: 18377911]
9. Liu C, Sun C, Huang H, Janda K, Edgington T. Overexpression of legumain in tumors is significant for invasion/metastasis and a candidate enzymatic target for prodrug therapy. *Cancer Res.* 2003; 63:2957–2964. [PubMed: 12782603]
10. Luo Y, Zhou H, Krueger J, Kaplan C, Lee SH, Dolman C, Markowitz D, Wu W, Liu C, Reisfeld RA, Xiang R. Targeting tumor-associated macrophages as a novel strategy against breast cancer. *J Clin Invest.* 2006; 116:2132–2141. [PubMed: 16862213]
11. Chan CB, Abe M, Hashimoto N, Hao C, Williams IR, Liu X, Nakao S, Yamamoto A, Zheng C, Henter JI, Meeths M, Nordenskjold M, Li SY, Hara-Nishimura I, Asano M, Ye K. Mice lacking asparaginyl endopeptidase develop disorders resembling hemophagocytic syndrome. *Proc Natl Acad Sci U S A.* 2009; 106:468–473. [PubMed: 19106291]
12. Kembhavi AA, Buttle DJ, Knight CG, Barrett AJ. The two cysteine endopeptidases of legume seeds: purification and characterization by use of specific fluorometric assays. *Arch Biochem Biophys.* 1993; 303:208–213. [PubMed: 8512309]
13. Niestroj AJ, Feussner K, Heiser U, Dando PM, Barrett A, Gerhartz B, Demuth HU. Inhibition of mammalian legumain by Michael acceptors and AzaAsn-halomethylketones. *Biol Chem.* 2002; 383:1205–1214. [PubMed: 12437107]
14. Sexton KB, Witte MD, Blum G, Bogyo M. Design of cell-permeable, fluorescent activity-based probes for the lysosomal cysteine protease asparaginyl endopeptidase (AEP)/legumain. *Bioorg Med Chem Lett.* 2007; 17:649–653. [PubMed: 17189693]
15. Kato D, Boatright KM, Berger AB, Nazif T, Blum G, Ryan C, Chehade KA, Salvesen GS, Bogyo M. Activity-based probes that target diverse cysteine protease families. *Nat Chem Biol.* 2005; 1:33–38. [PubMed: 16407991]
16. Rozman-Pungercar J, Kopitar-Jerala N, Bogyo M, Turk D, Vasiljeva O, Stefe I, Vandenabeele P, Bromme D, Puizdar V, Fonovic M, Trstenjak-Prebanda M, Dolenc I, Turk V, Turk B. Inhibition of papain-like cysteine proteases and legumain by caspase-specific inhibitors: when reaction mechanism is more important than specificity. *Cell Death Differ.* 2003; 10:881–888. [PubMed: 12867995]
17. Loak K, Li DN, Manoury B, Billson J, Morton F, Hewitt E, Watts C. Novel cell-permeable acyloxymethylketone inhibitors of asparaginyl endopeptidase. *Biol Chem.* 2003; 384:1239–1246. [PubMed: 12974392]



18. Edgington LE, Berger AB, Blum G, Albrow VE, Paulick MG, Lineberry N, Bogyo M. Noninvasive optical imaging of apoptosis by caspase-targeted activity-based probes. *Nat Med.* 2009; 15:967–973. [PubMed: 19597506]
19. Berger AB, Witte MD, Denault JB, Sadaghiani AM, Sexton KM, Salvesen GS, Bogyo M. Identification of early intermediates of caspase activation using selective inhibitors and activity-based probes. *Mol Cell.* 2006; 23:509–521. [PubMed: 16916639]
20. Kato D, Verhelst SH, Sexton KB, Bogyo M. A general solid phase method for the preparation of diverse azapeptide probes directed against cysteine proteases. *Org Lett.* 2005; 7:5649–5652. [PubMed: 16321013]
21. Joyce JA, Baruch A, Chehade K, Meyer-Morse N, Giraud E, Tsai FY, Greenbaum DC, Hager JH, Bogyo M, Hanahan D. Cathepsin cysteine proteases are effectors of invasive growth and angiogenesis during multistage tumorigenesis. *Cancer Cell.* 2004; 5:443–453. [PubMed: 15144952]
22. Asgian JL, James KE, Li ZZ, Carter W, Barrett AJ, Mikolajczyk J, Salvesen GS, Powers JC. Azapeptide epoxides: a new class of inhibitors selective for clan CD cysteine proteases. *J Med Chem.* 2002; 45:4958–4960. [PubMed: 12408706]
23. Shirahama-Noda K, Yamamoto A, Sugihara K, Hashimoto N, Asano M, Nishimura M, Hara-Nishimura I. Biosynthetic processing of cathepsins and lysosomal degradation are abolished in asparaginyl endopeptidase-deficient mice. *J Biol Chem.* 2003; 278:33194–33199. [PubMed: 12775715]
24. Blum G, von Degenfeld G, Merchant MJ, Blau HM, Bogyo M. Noninvasive optical imaging of cysteine protease activity using fluorescently quenched activity-based probes. *Nat Chem Biol.* 2007; 3:668–677. [PubMed: 17828252]
25. Lennon-Dumenil AM, Bakker AH, Maehr R, Fiebiger E, Overkleeft HS, Roseblatt M, Ploegh HL, Lagaudriere-Gesbert C. Analysis of protease activity in live antigen-presenting cells shows regulation of the phagosomal proteolytic contents during dendritic cell activation. *J Exp Med.* 2002; 196:529–540. [PubMed: 12186844]
26. Fischer R, Fotin-Mleczek M, Hufnagel H, Brock R. Break on through to the other side—biophysics and cell biology shed light on cell-penetrating peptides. *Chembiochem.* 2005; 6:2126–2142. [PubMed: 16254940]
27. Mintzer MA, Simanek EE. Nonviral vectors for gene delivery. *Chem Rev.* 2009; 109:259–302. [PubMed: 19053809]
28. Rajendran L, Schneider A, Schlechtingen G, Weidlich S, Ries J, Braxmeier T, Schwille P, Schulz JB, Schroeder C, Simons M, Jennings G, Knolker HJ, Simons K. Efficient inhibition of the Alzheimer's disease beta-secretase by membrane targeting. *Science.* 2008; 320:520–523. [PubMed: 18436784]
29. Sexton KB, Kato D, Berger AB, Fonovic M, Verhelst SH, Bogyo M. Specificity of aza-peptide electrophile activity-based probes of caspases. *Cell Death Differ.* 2007; 14:727–732. [PubMed: 17170749]

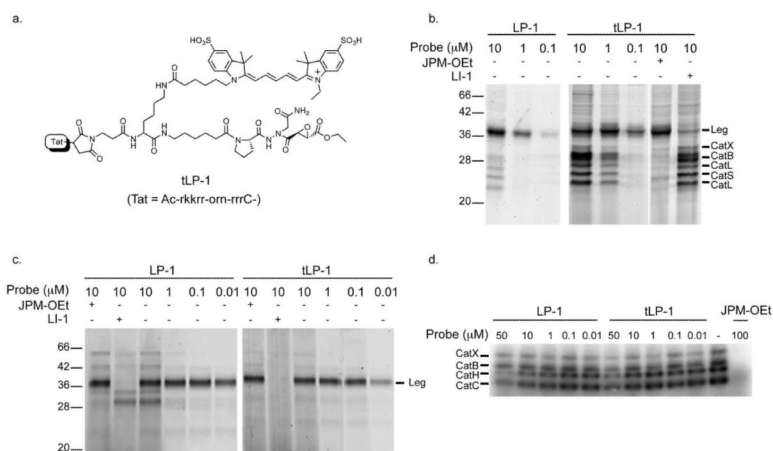


**Figure 1.** Legumain inhibitors and probes (a) Structures of Aza-Asn epoxide legumain inhibitor, LI-1 and legumain probe, LP-1 compared to Asp-AOMK inhibitor, LI-0 and probe, LP-0. (b) Direct labeling of legumain in intact cells by LP-1 and LP-0. Intact monolayers of NIH-3T3 fibroblasts (top) or RAW 264.7 macrophages (bottom) were pre-treated with the cathepsin inhibitor JPM-OEt (10  $\mu$ M; first column), the legumain inhibitors LI-0/LI-1 (10  $\mu$ M; second and third columns) and labeled by addition of LP-1 and LP-0 at the indicated concentrations.

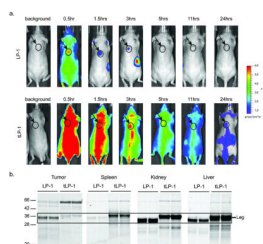


**Figure 2.**

(a) *In vivo* imaging of active legumain. Mice bearing C2C12/ras xenograft tumors were IV injected with LP-1 (top) or LP-1-ctrl (bottom) probes and mice imaged at the indicated time points. Images are presented using a colorimetric scale based on photons per second per centimeter square per steradian ( $\text{p s}^{-1} \text{cm}^{-2} \text{sr}^{-1}$ ) overlaid on bright light images. (b) Tumor to normal tissue signal ratio calculated from the mice labeled with LP-1 (circle symbols with a solid line) and LP-1 Ctrl (square symbols with a dotted line). Ratios were calculated from multiple mice ( $n = 3$  for LP-1 and  $n = 2$  for LP-1 Ctrl) and represent mean  $\pm$  standard error. (c) Ex-vivo imaging of organs and protein labeling analyzed by SDS-PAGE. Fluorecently labeled proteins were visulaized by scanning of the gel using a flatbed laser scanner. Each column represents an organ from individual mouse collected after *in vivo* imaging experiments.

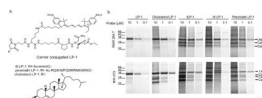
**Figure 3.**

(a) Structure of tat-conjugated LP-1 (tLP-1) (b) Direct labeling of legumain in intact RAW 264.7 macrophages with LP-1 and tLP-1. Due to the differences in molecular weight between the two probes (approximately 1800), tLP-1 labeled legumain is slightly shifted on the gel relative to LP-1 labeled legumain. Where indicated, cells were pretreated with either the general cathepsin inhibitor JPM-OEt or the legumain specific inhibitor LI-1. (c) Comparison of labeling legumain in RAW cell lysates by LP-1 and tLP-1. (d) Competitive inhibition of cathepsins by LP-1 and tLP-1. RAW cell lysates were pre-treated with LP-1 and tLP-1 at the indicated concentrations and labeled by the general cathepsin probe  $^{125}\text{I}$ -DCG04.



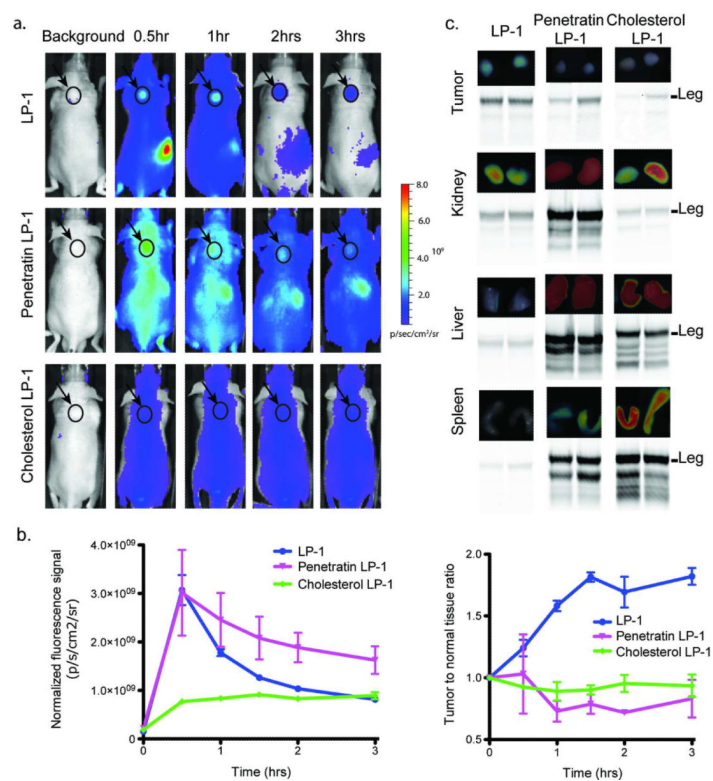
**Figure 4.**

(a) *In vivo* imaging of legumain using LP-1 and tLP-1. Mice bearing C2C12/ras xenograft tumors were IV injected with LP-1 (top) or tLP-1 (bottom) probes and mice imaged at the indicated time points. Images are presented using a colorimetric scale based on photons per second per centimeter square per steradian ( $\text{p s}^{-1} \text{cm}^{-2} \text{sr}^{-1}$ ) overlaid on bright light images. (b) Biochemical characterization of *in vivo* labeled legumain. Fluorecently labeled proteins from tissue homogenates were visualized by scanning of the gel using a flatbed laser scanner. Each column represents an organ from an individual mouse collected after *in vivo* imaging experiments

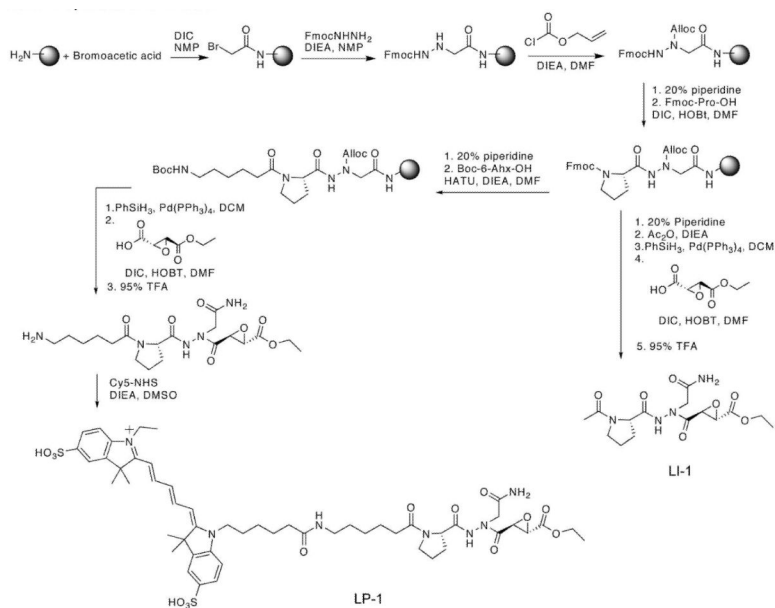


**Figure 5.**

(a) Structures of the carrier-conjugated activity-based probes. (b) Direct comparison between the carrier-conjugates. Intact RAW 264.7 macrophages (top) and NIH-3T3 fibroblasts (bottom) were labeled with each probe at the indicated concentrations. Total probe labeled proteins were visualized by SDS-PAGE followed by scanning of the gel using a flatbed laser scanner. The location of legumain (Leg) and cathepsins (Cat) are indicated

**Figure 6.**

(a) Comparison of *in vivo* fluorescent images of mice labeled with LP-1 and carrier-conjugated probes. Mice bearing C2C12/ras xenograft tumors were IV injected with LP-1 (top) or Penetratin LP-1 (middle) and Cholesterol LP-1 (bottom) probes and mice imaged at the indicated time points. Images are presented using a colorimetric scale based on photons per second per centimeter square per steradian ( $\text{p s}^{-1} \text{cm}^{-2} \text{sr}^{-1}$ ) overlaid on bright light images. (b) *Ex vivo* imaging of whole organs and SDS-PAGE analysis from the corresponding organ extracts. Fluorescent probe labeled proteins were visualized by scanning of the gel using a flatbed laser scanner. The location of legumain (Leg) is shown. (c) Quantification of fluorescent signal in tumors (left) compared to tumor to normal tissue signal ratios (right).



**Scheme 1.**  
Synthesis of LP-1 and LI-1



Table 1

Inhibition of various cysteine proteases by LI-1 and LI-0.

Inhibitor	Legumain		Cathepsin B		Cathepsin L		Caspase-3	
	IC <sub>50</sub>	k <sub>obs</sub> /[I]	IC <sub>50</sub>	IC <sub>50</sub>	IC <sub>50</sub>	IC <sub>50</sub>	IC <sub>50</sub>	IC <sub>50</sub>
LI-1	11.5nM	72352 M <sup>-1</sup> s <sup>-1</sup>	390 μM	220 μM	890 μM			
LI-0	704 nM	1586 M <sup>-1</sup> s <sup>-1</sup>	>1 mM	>1 mM	2.8 μM			
JPM-OEt <sup>a</sup>		N/D	0.78 μM	2.98 μM	N/D			
Z-DEVD-FMK <sup>b</sup>		N/D	N/D	N/D	0.13 μM			

<sup>a</sup>JPM-OEt is a broad-spectrum cathepsin inhibitor.

<sup>b</sup>Z-DEVD-FMK is a caspase-3 specific inhibitor.